*Materials Transactions*, Vol. 49, No. 11 (2008) pp. 2484 to 2490
Special Issue on Advances in Computational Materials Science and Engineering V


# First Principles Calculation of CO and $H_2$ Adsorption on Strained Pt Surface

Akihide Kuwabara[1], Yohei Saito[2], Yukinori Koyama[2], Fumiyasu Oba[2], Katsuyuki Matsunaga[1,2] and Isao Tanaka[1,2]

[1]*Nanostructures Research Laboratory, Japan Fine Ceramics Center, Nagoya 456-8587, Japan*
[2]*Department of Materials Science and Engineering, Kyoto University, Kyoto 606-8501, Japan*

First principles calculations are carried out to analyze adsorption of CO and $H_2$ molecules on a Pt (111) surface and the effect of surface strain on the adsorption energy. A CO molecule is more adsorptive on the Pt (111) surface than a $H_2$ molecule under an ordinary condition. Surface expansion enhances CO poisoning on a Pt (111) surface. On the contrary, a compressive strain reduces adsorptive strength of a CO molecule. Similar tendency is also found in adsorption of a $H_2$ molecule on the bridge, fcc-hollow, and hcp-hollow sites. However, $H_2$ adsorption on the top site is less affected by the strain. As a consequence, the difference of adsorption energies between CO and $H_2$ molecules becomes smaller when compressive strain is introduced into the Pt (111) surface. Based on thermodynamics, surface coverage ratio is quantitatively evaluated with taking into account the effect of surface strain and partial pressure of gas phase. It is revealed that compressive strain improves probability of $H_2$ adsorption on Pt surface. [doi:10.2320/matertrans.MB200817]

(Received May 20, 2008; Accepted July 24, 2008; Published October 8, 2008)

***Keywords:*** *first principles calculation, metal surface, adsorption, electrode*

## 1. Introduction

A polymer electrolyte fuel cell (PEFC) is expected as a clean source of electricity which can generate electrical power from $H_2$ and $O_2$ gases and emit only $H_2O$. Applications of PEFC cover wide areas such as electric vehicles and mobile devices because of high density of electrical power and low working temperature. Several problems, however, should be solved before achieving commercialization of PEFC. Electrode is one of the most challenging tasks. Basically, Pt is used for both of anode and cathode sides of PEFC. At the anode side, $H_2$ gas is adsorbed on surfaces of Pt electrode and is transformed into protons and electrons through catalysis promoted by Pt. A problem is caused by an impurity gas of CO the fuel gas contains. Even if contamination is the order of ppm, CO molecules almost fully cover the surface of Pt electrode and prevent $H_2$ fuel gas from reacting on Pt surface.[1)] Such loss of a catalytic function by a CO gas is known as CO poisoning. Alloying of Pt with transition metals[2)] is mainly adopted as a method to improve resistance against CO poisoning. Recently, surface strain is studied as a new factor to control adsorption of gas molecules on metal surfaces.[3–8)] It is meaningful to understand the effect of surface strain on adsorption reaction because surface strain occurs by surface segregation in alloys.

A main purpose of the present study is to investigate the effect of surface strain on adsorption behavior in a metallic system. For a simple analysis, we are first focusing on adsorption of $H_2$ and CO molecules on a Pt surface.

## 2. Computational Methodology

### 2.1 Ground state calculation

Ground state calculation was carried out by VASP code[9,10)] based on density functional theory (DFT).[11)] Electron-ion interaction was represented by the projector augmented wave (PAW) method.[12)] The generalized gradient approximation (GGA)[13)] is chosen for formalism of the exchange-correlation term. Configurations of valence electrons are $5d^9\ 6s^1$ for Pt, $1s^1$ for H, $2s^2\ 2p^2$ for C, and $2s^2\ 2p^4$ for O. Basis functions include plane waves up to kinetic energies of 400 eV.

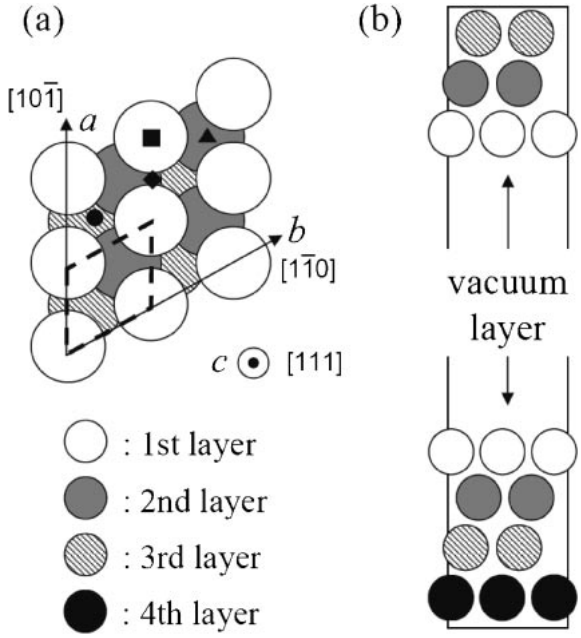


Fig. 1 (a) A top and (b) side view of the Pt (111) slab model in this study. In the panel (a), a red broken line indicates a unit cell of the (111) plane. Adsorption sites of top, bridge, fcc-hollow, and hcp-hollow are shown as filled marks, ■, ◆, ▲ and ●, respectively.

In the present study, a (111) surface of Pt is studied. Figure 1 shows our slab model. This model is 2×2 of a (111) surface primitive unit constructed from an optimized unit cell of Pt bulk ($a = 3.977$ Å), and includes 2 surfaces, 7 layers of Pt, and a vacuum layer with a thickness of 17 Å. **k** point sampling in the Brillouin zone was based on the Monkhorst-Pack scheme[14)] and mesh size of the sampling was 7×7×1. This set satisfies that convergence of calculated surface energy against number of sampling points becomes

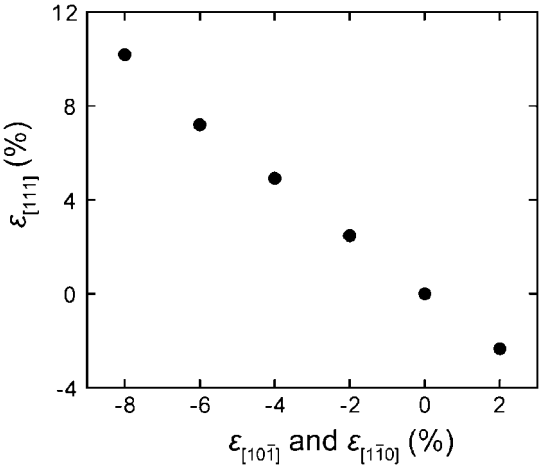


Fig. 2 A plot of elongation of atomic layer distance in the [111] direction to a surface strain in a (111) plane.

lower than 1 meV/Å$^2$. Before adsorption, structural relaxation was carried out for a clean surface. In order to keep a bulk-like region in the slab model, atomic positions of 3 layers in the middle were always fixed during geometry optimization. Relaxation for a clean surface was stopped after that Hellmann-Feynman forces become smaller than 0.02 eV/Å. In calculations of adsorption, a molecule was put in a vacuum region with an initial distance of 2 Å between the molecule and the first layer of Pt surface. All atomic positions except the 3 layers in the middle of the slab were optimized with the same condition as that for the clean surface.

In order to analyze the effect of a surface strain on adsorption behavior, strained-surface models were constructed. Lattice constants of a surface unit cell in the $a$ and $b$ directions, $[10\bar{1}]$ and $[1\bar{1}0]$ as is shown in Fig. 1, respectively, were simultaneously expanded (or shrunk) with the same strain, $\varepsilon$. $\varepsilon$ is given as

$$\varepsilon = \Delta l / l_0 \tag{1}$$

where $l_0$ is a lattice constant under an ordinary condition and $\Delta l$ is a change in the length of the lattice constant. Strains in the $[10\bar{1}]$ and $[1\bar{1}0]$ direction, $\varepsilon_{[10\bar{1}]}$ and $\varepsilon_{[1\bar{1}0]}$, vary from $-6\%$ to $+2\%$ and $\varepsilon_{[10\bar{1}]}$ is always equal to $\varepsilon_{[1\bar{1}0]}$. The stable lattice constant in the $c$ direction, [111], of the Pt (111) surface unit cell needed to be determined for each of strain in the $a$ and $b$ directions. For this purpose, total energy calculations of several surface models with varying a distance between atomic layers were performed at a respective strain in the $a$ and $b$ directions. Figure 2 shows a relationship between $\varepsilon_{[111]}$ and $\varepsilon_{[10\bar{1}]}$.

### 2.2 Adsorption Gibbs free energy and coverage ratio

Now, we are focusing on the following adsorption reaction of a gas species of $i$ on a surface of $X$,

$$v_{\mathrm{ads}} + i(g) \rightarrow i_{\mathrm{ads}} \tag{2}$$

$v_{\mathrm{ads}}$ is a vacant adsorption site on a surface and $i_{\mathrm{ads}}$ is an adsorbed species of $i$. Fractions of the sites of $v_{\mathrm{ads}}$ and $i_{\mathrm{ads}}$, $[v_{\mathrm{ads}}]$ and $[i_{\mathrm{ads}}]$, can be represented by the adsorption Gibbs free energy per one adsorbate particle, $\Delta G^{i,X}_{\mathrm{ads}}$, as

$$\frac{[i_{\mathrm{ads}}]}{[v_{\mathrm{ads}}]} = \exp\left(-\frac{\Delta G^{i,X}_{\mathrm{ads}}}{k_{\mathrm{B}}T}\right). \tag{3}$$

Derivation of eq. (3) is shown in Appendix section. According to a limit of total site number,

$$[v_{\mathrm{ads}}] + \sum_i [i_{\mathrm{ads}}] = 1. \tag{4}$$

We finally obtain coverage ratio by $i$ as

$$\theta_i = \frac{\exp\left(-\dfrac{\Delta G^{i,X}_{\mathrm{ads}}}{k_{\mathrm{B}}T}\right)}{1 + \displaystyle\sum_i \exp\left(-\frac{\Delta G^{i,X}_{\mathrm{ads}}}{k_{\mathrm{B}}T}\right)}. \tag{5}$$

In eq. (5), $[i_{\mathrm{ads}}]$ is expressed as $\theta_i$. In order to evaluate a surface coverage ratio, we have to know a value of $\Delta G^{i,X}_{\mathrm{ads}}$. $\Delta G^{i,X}_{\mathrm{ads}}$ is given by the following equation,

$$\Delta G^{i,X}_{\mathrm{ads}} = G_{X-i} - (G^X_{\mathrm{surf}} + G^i_{\mathrm{gas}}). \tag{6}$$

$G_{X-i}$ is a Gibbs free energy of a surface adsorbed by a gas molecule (or atom). $G^X_{\mathrm{surf}}$ and $G^i_{\mathrm{gas}}$ are Gibbs free energies of a clean surface and a gas molecule (or atom), respectively. In this description, adsorptive species shows negative $\Delta G^{i,X}_{\mathrm{ads}}$. When adsorption strength becomes stronger, $\Delta G^{i,X}_{\mathrm{ads}}$ becomes more negative. Equation (6) indicates that $\Delta G^{i,X}_{\mathrm{ads}}$ depends on a chemical potential of a gaseous phase. Assuming that the gaseous phase is an ideal gas, $G^i_{\mathrm{gas}}$ at a temperature ($T$) and a partial pressure ($p_i$) is expressed as

$$G^i_{\mathrm{gas}} = G^\circ_{\mathrm{gas}}(p^\circ, T) + k_{\mathrm{B}}T \ln \frac{p_i}{p^\circ}, \tag{7}$$

where $G^\circ_{\mathrm{gas}}(p^\circ, T)$ is a standard Gibbs free energy of the gaseous phase at a temperature $T$ and a standard pressure $p^\circ$, 1 atm. $G^\circ_{\mathrm{gas}}(p^\circ, T)$ can be given by enthalpy and entropy as

$$\begin{aligned} G^\circ_{\mathrm{gas}}(p^\circ, T) = {} & H^\circ_{\mathrm{gas}}(p^\circ, 0\,\mathrm{K}) + \Delta H^\circ_{\mathrm{gas}}(p^\circ, T) \\ & - T \cdot S^\circ(p^\circ, T). \end{aligned} \tag{8}$$

$H^\circ_{\mathrm{gas}}(p^\circ, 0\,\mathrm{K})$ and $\Delta H^\circ_{\mathrm{gas}}(p^\circ, T)$ are an enthalpy at 0 K and a temperature dependence term of the enthalpy, respectively. $S^\circ(p^\circ, T)$ is an entropy. In this study, we assumed that a total energy of a gas molecule obtained by DFT calculation ($E^i_{\mathrm{gas}}$) can be substituted for $H^\circ_{\mathrm{gas}}(p^\circ, 0\,\mathrm{K})$. If the values of $\Delta H^\circ_{\mathrm{gas}}(p^\circ, T)$ and $S^\circ(p^\circ, T)$ were referred from the tables of thermochemical data,[15] $G^i_{\mathrm{gas}}$ at any given temperatures and partial pressures of a gas phase can be obtained through DFT calculations. In the present study, $G_{X-i}$ and $G^X_{\mathrm{surf}}$ are substituted for the total energies of DFT calculations using a slab model with clean and adsorbed surfaces, $E_{X-i}$ and $E^X_{\mathrm{surf}}$, respectively. Thus, the effects of vibrational entropies for these terms are not taken into account on the assumption that temperature dependence of $G_{X-i}$ and $G^X_{\mathrm{surf}}$ are negligible compared to that of $G^i_{\mathrm{gas}}$. $\Delta G^{i,X}_{\mathrm{ads}}$ of eq. (6) can be rewritten as

$$\begin{aligned} \Delta G^{i,X}_{\mathrm{ads}} = {} & G_{X-i} - \Big(G^X_{\mathrm{surf}} + H^\circ_{\mathrm{gas}}(p^\circ, 0\,\mathrm{K}) \\ & + \Delta H^\circ_{\mathrm{gas}}(p^\circ, T) - T \cdot S^\circ(p^\circ, T) + k_{\mathrm{B}}T \ln \frac{p_i}{p^\circ}\Big) \\ \cong {} & \{E_{X-i} - (E^X_{\mathrm{surf}} + E^i_{\mathrm{gas}})\} \\ & - \left(\Delta H^\circ_{\mathrm{gas}}(p^\circ, T) - T \cdot S^\circ(p^\circ, T) + k_{\mathrm{B}}T \ln \frac{p_i}{p^\circ}\right). \end{aligned} \tag{9}$$

The first term in eq. (9) is an energy difference between before and after adsorption, which can be obtained by DFT calculations. We simply call this term as "adsorption energy". It should be emphasized that this term is distinguished from the adsorption Gibbs free energy, $\Delta G^{i,X}_{\mathrm{ads}}$, in this study. The second term is temperature and partial pressure dependence in $G^{i}_{\mathrm{gas}}$. Finally, we can simply express eq. (9) as the following,

$$\Delta G^{i,X}_{\mathrm{ads}} = \Delta E^{i,X}_{\mathrm{ads,DFT}} - \Delta G^{i}_{\mathrm{gas}}(T, p). \tag{10}$$

$\Delta G^{i,X}_{\mathrm{ads}}$ is clearly dependent on a temperature and a partial pressure of a gas phase. $\theta_i$ is affected by a temperature and a partial pressure because of the dependence of $\Delta G^{i,X}_{\mathrm{ads}}$ on these parameters.

## 3. Results and Discussion

### 3.1 Adsorption of a CO molecule

In the adsorption of a CO molecule on Pt (111) surface, the C atom side directly contacts with Pt surface. The direction of C-O bonding is vertical to the (111) plane of Pt. Table 1 summarizes our results of adsorption energy of a CO molecule ($\Delta E^{\mathrm{CO,Pt}}_{\mathrm{ads,DFT}}$) on different adsorption sites. From the viewpoint of symmetry, there are 4 different adsorption sites on Pt (111) surface as shown in Fig. 1. They are called as "top", "bridge", "fcc-hollow", and "hcp-hollow". In the experiment, the top site is the most stable site for CO adsorption.[20] However, our calculation shows that the hollow site is the lowest adsorption energy. Similar contradictions have been widely reported in the DFT study about CO adsorption on Pt surface.[21] Kresse *et al.* have recently reported that preference of CO adsorption on Pt surface can be correctly predicted by the GGA + $U$ method.[22] Their calculation reveals that the energy gap between the highest occupied molecular orbital (HOMO) and the lowest unoccupied molecular orbital (LUMO) of a CO molecule should be accurately estimated for CO adsorption on a Pt surface. Doll has proposed a similar conclusion through hybrid functional calculations.[16] Philipsen *et al.* compared relativistic and non-relativistic calculations based on a frozen core approximation. As is shown in Table 1, they found that relativistic calculation is successful to reproduce preference of CO adsorption on Pt similar to experiments.[17] Orita *et al.* also performed all electron relativistic (AER) calculation and have concluded that lower Fermi energy in AER calculations is attributed to the correct estimation of the site dependence of CO adsorption.[23] Failure in preference of adsorption site by the ordinary DFT calculations is thought to result from the overestimation of interaction between Pt 5*d* state and $2\pi$ orbital, which is the LUMO, of a CO molecule. Accurate prediction of adsorption site of CO molecule is beyond our main purpose in the present article. The calculated adsorption energy at the top site has an error of 0.17∼0.34 eV in comparison with experimental reports.[18,19] With regard to CO adsorption, we focus only on CO adsorption at the top site in the latter part of this article.

Table 1 Adsorption energy of a CO molecule on the Pt (111) surface. All of the values in this table are expressed by a unit of eV. FR, NR, AER, and AENR mean full relativistic, non-relativistic, all electron relativistic, and all electron non-relativistic calculations, respectively.

| | top | bridge | fcc-hollow | hcp-hollow |
|---|---|---|---|---|
| Present work | −1.67 | −1.79 | −1.81 | −1.80 |
| Calc. (GGA)*1 | −1.64 | −1.67 | −1.74 | −1.72 |
| Calc. (B3LYP)*1 | −1.44 | −1.38 | −1.40 | −1.34 |
| Calc. (FR, GGA)*2 | −1.29 | | | −1.05 |
| Calc. (NR, GGA)*2 | −0.83 | | | −1.02 |
| Calc. (AER, GGA)*3 | −1.94 | −1.85 | −1.80 | −1.77 |
| Calc. (AENR, GGA)*3 | −0.93 | (not stable) | −1.42 | −1.38 |
| Exp.*4 | −1.33 | | | |
| Exp.*5 | −1.50 | | | |

*1Ref. 16) *2Ref. 17) *3Ref. 23) *4Ref. 18) *5Ref. 19)

Figure 3 shows projected local density of states (DOS) of C, O, and Pt atoms at the 1st layer of a slab obtained from Pt slab models including a CO molecule. The CO molecule is put into a vacuum layer far from the surface and is adsorbed on the top site of a Pt (111) surface in Fig. 3(a) and (b), respectively. With regard to Fig. 3(b), only the DOS of the Pt atom bound with the C atom are shown. Fermi energy is set to be 0 eV in these graphs. As shown in Fig. 3(a), DOS from C and O atoms indicate strong localization and are overlapped with each other because they form molecular orbitals. These molecular orbitals are labeled as $3\sigma$, $4\sigma$, $1\pi$, $5\sigma$, and $2\pi$ from lower to higher energy. $5\sigma$ and $2\pi$ are the HOMO and the LUMO, respectively, of an isolated CO molecule. No interaction can be found between the CO molecule and Pt substrate in Fig. 3(a) because the CO molecule is far away from the Pt surface in our clean-surface model. Absorption of the CO molecule on the Pt surface obviously changes DOS profiles. The orbitals of CO molecule hybridize with Pt 5*d* and 6*s* states. The hybridization shifts $4\sigma$, $1\pi$ and $5\sigma$ orbitals to lower energy. DOS of Pt have sharp peaks at the same energy as these orbitals of the CO molecule. With regard to the LUMO of $2\pi$ orbital, unoccupied states located at 3 eV become broaden due to interaction with Pt 5*d*. In addition, the $2\pi$ orbital has extra gap states between −5 to 0 eV.

### 3.2 Adsorption of a hydrogen atom

Our calculations show that a $H_2$ molecule is always dissociated into two H atoms on Pt surface through geometry optimization. This is independent on where $H_2$ molecule is initially located on a Pt (111) surface. Based on this result, adsorption of a hydrogen atom is alternatively calculated for the purpose of reducing calculation times related to dissociation of a $H_2$ molecule. Adsorption energy of a $H_2$ molecule as expressed in eq. (10), $\Delta E^{\mathrm{H_2,Pt}}_{\mathrm{ads,DFT}}$, is calculated by the following equation,

$$\Delta E^{\mathrm{H_2,Pt}}_{\mathrm{ads,DFT}} = 2E_{\mathrm{Pt\text{-}H}} - (E_{\mathrm{Pt+H_2}} + E_{\mathrm{Pt}}), \tag{11}$$

where $E_{\mathrm{Pt\text{-}H}}$, $E_{\mathrm{Pt+H_2}}$, and $E_{\mathrm{Pt}}$ are the energy of a Pt slab with an adsorbed H atom, a Pt slab with a $H_2$ molecule in a vacuum layer, and a pure Pt slab.

Table 2 shows calculated adsorption energies of a $H_2$ molecule on each of adsorption sites. Adsorption energies on the top, bridge, and hcp-hollow sites are almost same. The most stable adsorption site is the fcc-hollow site. This is coincident with the experimental result.[27] As is mentioned before, the relativistic calculations are successful to evaluate

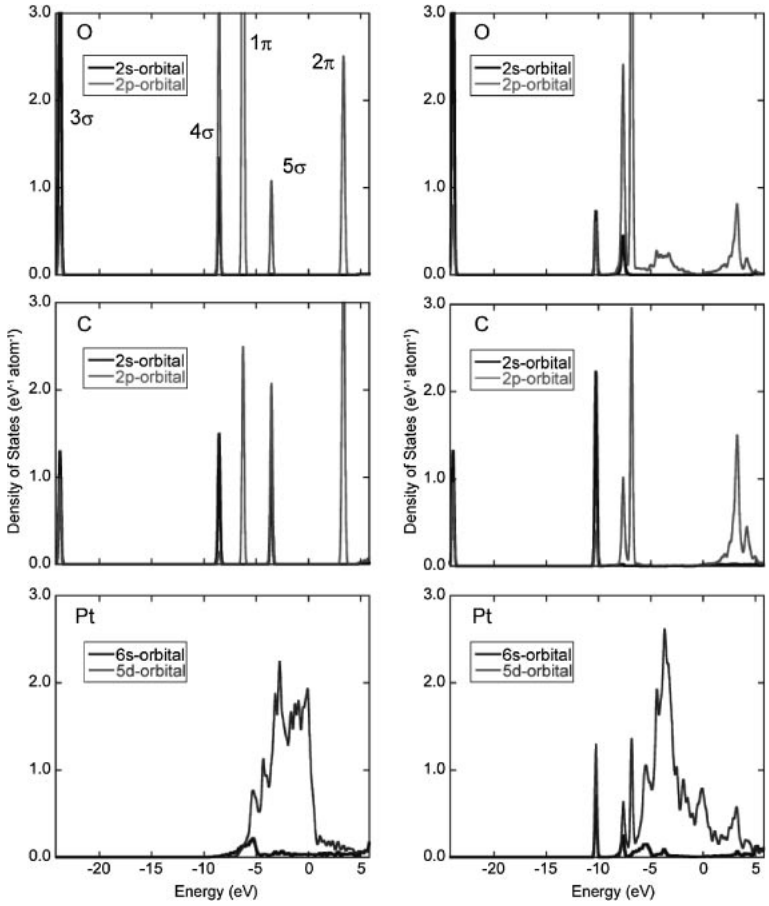


Fig. 3 Projected local density of states from Pt slab models (left side) with clean surfaces and a CO molecule in a vacuum layer and (right side) with a CO-adsorbed surface.

Table 2 Adsorption energy of a $H_2$ molecule on the Pt (111) surface. All of the values in this table are expressed by a unit of eV.

| | top | bridge | fcc-hollow | hcp-hollow |
|---|---|---|---|---|
| Present work | −0.97 | −0.94 | −1.03 | −0.95 |
| Calc.*1 | −0.90 | | −0.98 | −0.90 |
| Calc. (SR, GGA)*2 | −0.42 | | −0.33 | |
| Calc. (NR, GGA)*2 | 0.19 | | −0.09 | |
| Exp.*3 | | | −0.78 | |

*1Ref. 24) *2Ref. 25) *3Ref. 26)

preference site of CO adsorption.[17,23] With regard to $H_2$ adsorption, Olsen *et al.* reported that their relativistic calculations have contradiction with the preferable site of hydrogen on Pt.[25] Similar to the adsorption energy of a CO molecule, the adsorption energy of a $H_2$ molecule is overestimated in comparison with an experimental report.[26] With regard to a difference of the adsorption energies between CO and $H_2$ molecule, the value of our calculation, 0.64 eV, is fairly comparable to that of experiment, 0.55–0.72 eV.

Figure 4 show projected local DOS of H and Pt atoms at the 1st surface layer before and after hydrogen adsorption on Pt (111) surface. The $H_2$ molecule is put into a vacuum region far from the surface in the model corresponding to Fig. 4(a). Adsorption site of a hydrogen atom is the fcc-hollow site. In Fig. 4(b), only the local DOS of the Pt atoms bonding with an adsorbed H atom are shown. Chemical bonding changes in adsorption of a H atom seems to be simple compared to the adsorption of a CO molecule. When the $H_2$ molecule is far from Pt surface, there is a sharp peak attributed to a bonding molecular orbital of $H_2$ at around −4 eV. After adsorption and dissociation into H atoms, the peak of H 1*s* shifts down to −8 eV and becomes broader. This is due to hybridization with Pt 5*d* and 6*s*.

### 3.3 Strain effect on adsorption energy

Figure 5 shows dependence of the adsorption energy on surface strain. As shown in Fig. 5(a), the adsorption energy of a CO molecule obviously shows negative linear relationship to the surface strain. Compressive surface strain makes the adsorption energy of a CO molecule less negative, namely CO adsorption becomes weaker. With regard to adsorption of a $H_2$ molecule, compressive strain also reduces adsorptive abilities on the bridge, fcc-hollow, and hcp-hollow sites. On the contrary, adsorption of a $H_2$ molecule on the top site is less affected by the strain. The most stable adsorption site for a $H_2$ molecule changes from the fcc-hollow to the top site when compressive strain is larger than 2%. As a result, the difference of adsorption energy between CO and $H_2$ molecules ($\Delta E_{ads}$) depends on the surface strain. $\Delta E_{ads}$ is defined as

$$\Delta E_{ads} = \min[\Delta E^{H_2,Pt}_{ads,DFT}] - \Delta E^{CO,Pt}_{ads,DFT}. \quad (12)$$

As shown in Fig. 5(c), $\Delta E_{ads}$ are always positive values within a whole range of strain. Adsorptive ability of a CO

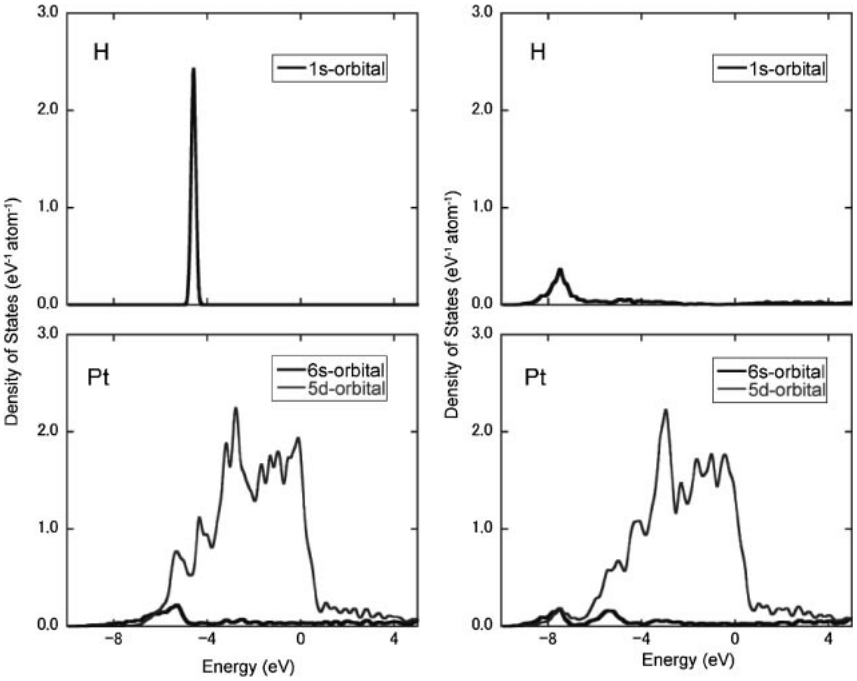


Fig. 4 Projected local density of states from Pt slab models (left side) with clean Pt surfaces and a $H_2$ molecule in a vacuum layer and (right side) with a H-adsorbed surface.

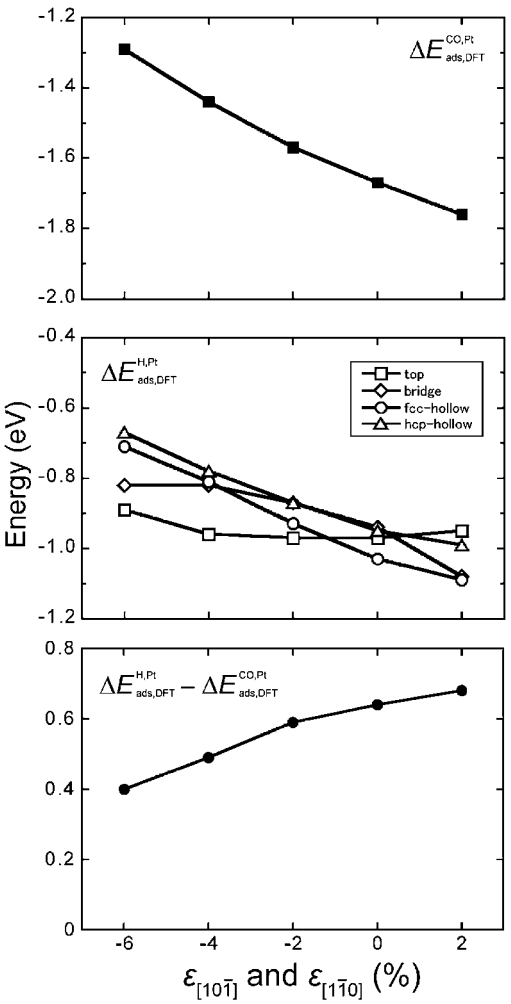


Fig. 5 Plots of CO adsorption energy, $\Delta E^{CO,Pt}_{ads,DFT}$, $H_2$ adsorption energy, $\Delta E^{H,Pt}_{ads,DFT}$, and difference between adsorption energies of CO and $H_2$, $\Delta E^{H,Pt}_{ads,DFT} - \Delta E^{CO,Pt}_{ads,DFT}$, to surface strain.

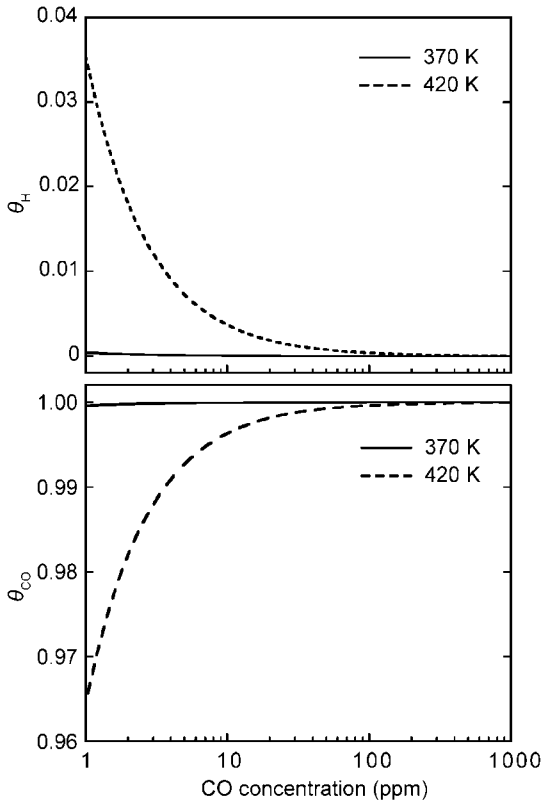


Fig. 6 Dependence of coverage ratio of H and CO on CO concentration in atmospheres at 370 and 420 K and wituout surface strain.

molecule is always higher than a $H_2$ molecule. However, the difference becomes smaller with increasing of compressive strain. Compressive strain is expected to suppress CO poisoning somehow.

In order to quantitatively estimate the effect of surface strain on CO poisoning, surface coverage ratio of CO

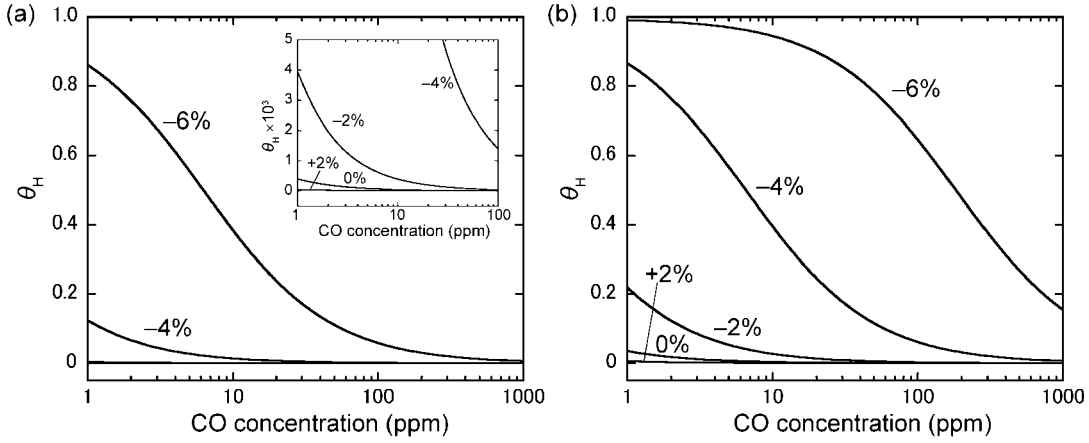


Fig. 7 Plots of H coverage ratio on strained Pt(111) surfaces to CO concentration in atmospheres at (a) 370 and (b) 420 K.

molecules and H atoms, $\theta_{CO}$ and $\theta_H$, are evaluated by eq. (5). Figure 6 shows dependence of $\theta_H$ and $\theta_{CO}$ on a concentration of CO gas in an atmosphere at 370 and 420 K. The results are obtained from the calculations of slab models without surface strain. The partial pressure of $H_2$ is set to be 1 atm. Even if the CO concentration is 1 ppm, Pt surface is fully covered by CO molecules at 370 K. A higher temperature of 420 K slightly increases the coverage ratio of H atoms and the coverage ratio of H atoms reaches only 3.5% at most. Temperature effect seems to be negligible under the ordinary condition. Figure 7 is graphs of relationship between $\theta_H$ and CO concentrations on strained Pt surfaces at 370 and 420 K. $\theta_H$ increases with increasing of compressive surface strains. The compressive strain of 6% results in $\theta_H$ of 40 and 80% at CO concentrations of 10 and 1 ppm, respectively, at 370 K. If the temperature becomes 420 K, $\theta_H$ is more improved with compressive strain on surface. The compressive strain is well effective to suppress CO-poisoning. Schalapka *et al.* has reported that hetero-epitaxial Pt layer grown on Ru(0001) becomes less reactive to CO molecules.[28] They concluded that compressive strain acting on Pt layer is attributed to decrease of CO adsorption. Our results are coincident with their experimental results.

Improvement of $\theta_H$ by compressive strains is attributed to decreasing adsorption energy, namely less negative $\Delta E_{ads,DFT}^{CO,Pt}$. As mentioned before, the interaction between CO and Pt mainly results from hybridization of Pt 5*d* state with the $2\pi$ LUMO of a CO molecule. Needless to say, surface strain never affects the electronic structure of a CO molecule. Therefore, it is reasonable to suppose that weakening of CO adsorption is originated from the electronic state of the Pt surface. In Fig. 8, energy levels of weight centers of Pt 5*d* states in Pt clean surface models are plotted as a function of surface strain. The energy level of Pt 5*d* is measured from that of the $2\pi$ orbital of a CO molecule in a vacuum layer. Relative energy of the Pt 5*d* to the $2\pi$ orbital has linear relation to the surface strain. The energy level of Pt 5*d* state becomes deeper to the $2\pi$ orbital with compressive strain. A deeper Pt 5*d* state is unlikely to interact with the $2\pi$ orbital. It can be supposed that down shift of Pt 5*d* states with surface compression leads to reduce the adsorption energy of a CO molecule on Pt surface.

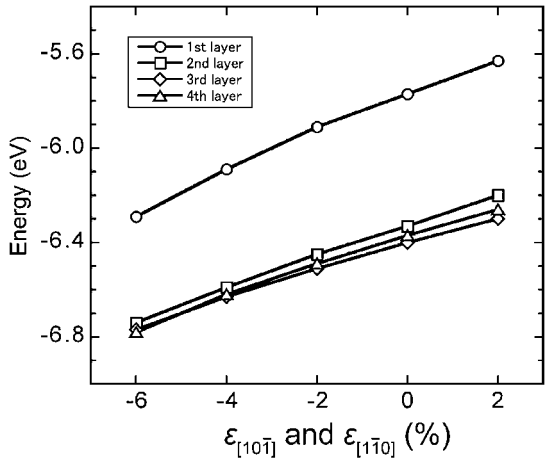


Fig. 8 Dependence of energy level of weight center of Pt 5*d* states on surface strain. The energy level is measured from the $2\pi$ orbital of a CO molecule in a vacuum layer of a slab model.

## 4. Conclusion

Total energy calculations based on density functional theory have been performed to investigate adsorption mechanism of CO and $H_2$ molecules on strained Pt (111) surfaces. The influence of surface strain on the adsorption has been quantitatively estimated by surface coverage ratio of CO and $H_2$ molecules. Our calculation reveals that a CO molecule becomes less adsorptive on Pt surface when compressive strain is applied to the surface. Surface strain also affects adsorption of $H_2$ similarly to the case of CO except that the adsorption of $H_2$ at the top site is less influenced. As a result, difference of adsorption energy between CO and $H_2$ molecule become smaller with increasing of compressive strain. The calculation of CO and H coverage ratio shows that Pt surface is fully covered by CO molecules under the ordinary condition. The phenomenon of CO poisoning is well reproduced. The surface ratio of H atoms is less than 0.1% even at 1 ppm CO in a gas phase. Compressive surface strain of −6% improve surface coverage ratio of $H_2$ up to 40% under the condition of 10 ppm CO and 100 K. The present results strongly indicate that surface

strain is an important parameter to control adsorption of gas molecules on Pt surface.

**Acknowledgment**

This work was financially supported by the New Energy and Industrial Technology Development Organization (NEDO) of Japan.

**Appendix**

We consider a surface of metal $X$ where a total number of adsorption site is $N$. Now, $n$ sites are occupied by adsorbate particles of a gaseous species $i$. Thus, a number of free sites is $N-n$. Total difference of a Gibbs energy from a clean surface is

$$\Delta G = n\Delta G^{i,X}_{\mathrm{ads}} - T\Delta S_{\mathrm{conf}} \tag{A·1}$$

$\Delta G^{i}_{\mathrm{ads}}$ is a Gibbs free energy to form one adsorbate particle of $i$ on the surface of $X$. $\Delta S_{\mathrm{conf}}$ is an entropy of configuration and is given as

$$\Delta S_{\mathrm{conf}} = k_{\mathrm{B}} \ln W, \tag{A·2}$$

where $W$ is a number of configurations. When $n$ sites is occupied and $(N-n)$ sites is free, the number of configuration is

$$W = \frac{N!}{n!(N-n)!}. \tag{A·3}$$

$\Delta S_{\mathrm{conf}}$ can be expressed as

$$\Delta S_{\mathrm{conf}} = k_{\mathrm{B}}\{\ln N! - \ln n! - \ln(N-n)!\}. \tag{A·4}$$

Equation (A·3) can be rewritten by the Stirling's formula, $\ln X! = X\ln X - X$, as

$$\begin{aligned}\Delta S_{\mathrm{conf}} &= k_{\mathrm{B}}[N\ln N - N - (n\ln n - n) \\ &\quad - \{(N-n)\ln(N-n) - (N-n)\}] \\ &= k_{\mathrm{B}}\{N\ln N - (N-n)\ln(N-n) - n\ln n\}\end{aligned} \tag{A·5}$$

Finally, eq. (A·1) becomes

$$\begin{aligned}\Delta G &= n\Delta G^{i,X}_{\mathrm{ads}} \\ &\quad - k_{\mathrm{B}}T\{N\ln N - (N-n)\ln(N-n) - n\ln n\}\end{aligned} \tag{A·6}$$

If a thermal equilibrium condition is achieved, $\Delta G$ as a function of $n$ has a local minimum, namely $\partial\Delta G/\partial n = 0$.

$$\begin{aligned}\frac{\partial \Delta G}{\partial n} &= \Delta G^{i,X}_{\mathrm{ads}} - k_{\mathrm{B}}T\ln\frac{N-n}{n} = 0 \\ \frac{n}{N-n} &= \exp\left(-\frac{\Delta G^{i,X}_{\mathrm{ads}}}{k_{\mathrm{B}}T}\right)\end{aligned} \tag{A·7}$$

Equation (A·7) can be expressed by fractions of occupied sites, $[i_{\mathrm{ads}}]$ $(= n/N)$, and of free sites, $[v_{\mathrm{ads}}]$ $(= (N-n)/N)$, as

$$\frac{n}{N-n} = \frac{n/N}{(N-n)/N} = \frac{[i_{\mathrm{ads}}]}{[v_{\mathrm{ads}}]} = \exp\left(-\frac{\Delta G^{i,X}_{\mathrm{ads}}}{k_{\mathrm{B}}T}\right) \tag{A·8}$$

**REFERENCES**

1) H. Igarashi, T. Fujino and M. Watanabe: J. Electroanal. Chem. **391** (1995) 119–123.
2) H. Igarashi, T. Fujino, Y. Zhu, H. Uchida and M. Watanabe: Phys. Chem. Chem. Phys. **3** (2001) 306–314.
3) M. Mavrikakis, B. Hammer and J. K. Norskøv: Phys. Rev. Lett. **81** (1998) 2819–2822.
4) M. Mavrikakis, P. Stoltze and J. K. Norskøv: Catalysis. Lett. **64** (2000) 101–106.
5) S. Sakong and A. Groß: Surf. Sci. **525** (2003) 107–118.
6) J. R. Kitchin, J. K. Norskøv, M. A. Barteau and J. G. Chen: Phys. Rev. Lett. **93** (2004) 156801.
7) R. Otero, F. Calleja, V. M. García-Suárez, J. J. Hinarejos, J. de la Figuera, J. Ferrer, A. L. Vázquez de Parga and R. Miranda: Surf. Sci. **550** (2004) 65–72.
8) M. Tsukada and H. Kasai: Phys. Rev. B **73** (2006) 155405.
9) G. Kresse and J. Furthmüller: Phys. Rev. B **54** (1996) 11169–11186.
10) G. Kresse and J. Furthmüller: J. Comput. Mater. Sci. **6** (1996) 15–50.
11) W. Kohn and L. J. Sham: Phys. Rev. A **140** (1965) 1133–1138.
12) P. E. Blöchl: Phys. Rev. B **50** (1994) 17953–17979.
13) J. P. Perdew, K. Burke and M. Ernzerhof: Phys. Rev. Lett. **77** (1996) 3865–3868.
14) H. J. Monkhorst and J. D. Pack: Phys. Rev. B **13** (1976) 5188.
15) M. W. Chase Jr.: NIST-JANAF Thermochemical Tables 4th ed. (The American Institute of Physics for The National Institute of Standards and Technology, New York, 1998).
16) K. Doll: Surf. Sci. **573** (2004) 464–473.
17) P. H. T. Philipsen, E. van Lenthe, J. G. Snijders and E. J. Baerends: Phys. Rev. B **56** (1997) 13556–13562.
18) E. G. Seebauer, A. C. F. Kong and L. D. Schmidt: J. Vac. Sci. Technol. **5** (1987) 464–468.
19) H. Steininger, S. Lehwald and H. Ibach: Surf. Sci. **123** (1982) 264–282.
20) M. O. Pedersen, M. L. Bocquet, P. Sautet, E. Laegsgaard, I. Stensgaard and F. Besenbacher: Chem. Phys. Lett. **299** (1999) 403–409.
21) P. J. Feibelman, B. Hammer, J. K. Nørskov, F. Wagner, M. Scheffler, R. Stumpf, R. Watwe and J. Dumesic: J. Phys. Chem. B **105** (2001) 4018–4025.
22) G. Kresse, A. Gil and P. Sautet: Phys. Rev. B **68** (2003) 073401.
23) H. Orita, N. Itoh and Y. Inada: Chem. Phys. Lett. **384** (2004) 271–276.
24) Y. Okamoto: Chem. Phys. Lett. **405** (2005) 79–83.
25) R. A. Olsen, G. J. Kroes and E. J. Baerends: J. Chem. Phys. **24** (1999) 11155–11163.
26) K. Christmann: Surf. Sci. Rep. **9** (1988) 1–163.
27) K. M. Lui, Y. Kim, W. M. Lau and J. W. Rabalais: Appl. Phys. Lett. **75** (1999) 587–589.
28) A. Schlapka, M. Lischka, A. Groß, U. Käsberger and P. Jakob: Phys. Rev. Lett. **91** (2003) 016101.